Pipe organ buffet radiation patterns under different excitation strategies

Gonzalo Villegas Curulla, Elliot K Canfield-Dafilou, Piergiovanni Domenighini, Benoît Fabre, Christophe d'Alessandro, Brian F. G. Katz

ICA 2022
24th INTERNATIONAL CONGRESS ON ACOUSTICS
October 24(Mon) - 28(Fri), 2022 Gyeongju, Korea

PROCEEDINGS of the
24th International Congress on Acoustics

October 24 to 28, 2022 in Gyeongju, Korea

ABS-0886

Pipe organ buffet radiation patterns under different excitation strategies

Gonzalo VILLEGAS CURULLA[(1)]; Elliot K. CANFIELD-DAFILOU[(1)]; Piergiovanni DOMENIGHINI[(2)]; Benoit FABRE[(1)]; Christophe d'ALESSANDRO[(1)]; Brian F. G. KATZ[(1)*]

[(1)]Sorbonne Université, CNRS, Institut Jean Le Rond d'Alembert, F-75005 Paris, France
[(2)]Università degli Studi di Perugia, Italy

ABSTRACT
Studying the directivity of musical instruments such as pipe organs is challenging because of their great size and because they typically cannot be moved from the locations where they are built to the laboratory. This study compares the radiation pattern of organ buffets under different excitation conditions, using a 19th century French pipe organ. We investigate the positive and the great organ independently due to their spatial separation and size. The excitation strategies were comprised of cylindrical and an omnidirectional electroacoustic sources. Measurements were carried out on each organ buffet along a horizontal line spanning the width of the church. Results in octave bands are shown and compared with a discussion on possible causes for observed differences. Significant variations in directivity were observed for the 2 kHz to 4 kHz octave-band regions where scattering from pipes is expected to have a predominant effect, while little variation from omnidirectional was observed for lower frequency bands for both sources.

Keywords: Pipe Organ, Source Directivity, Musical Acoustics

1 INTRODUCTION AND MOTIVATION

The interest of studying the radiation and directivity patterns of pipe organs is framed within the broader scope of modeling the acoustic behavior of individual components of pipe organs (e.g., pipes, windchests, buffets) both alone and in combination with one another. These goals are both theoretical—for understanding the underlying behavior of the instrument, and applied to case of modeling historical instruments such as the Dallery organ of Chapelle Sorbonne and the instrument in Notre-Dame by Thierry, Clicquot, and Cavaillé-Coll. An overview of the broader context of pipe organ modelling can be found in [1]. Results from recent campaigns of measurements and simulations are presented here as well as in [2, 3, 4, 5].

The current study considers the organ buffet as an acoustic obstacle (diffraction/scattering element). Horizontal directivity patterns of the positive and great organ of St. Élisabeth are presented when excited by idealized electroacoustic sources located within the buffets. These sources include an omnidirectional point-source (3D) and a linear-array cylindrical source (2D). These two approaches offer simplifications of the acoustic radiation of pipes within the organ buffets.

Different time scales are involved in the production and radiation of sound produced by pipe organs. Starting from the aero-acoustic sound production in each pipe, the sound is first radiated inside the buffet, where the characteristic time is given by L_{buf}/c ($\sim$5 ms in the current case), where L_{buf} is the characteristic length of the buffet (height of the facade's slit) and c the propagation velocity of the sound . The next time scale is given by the room.

In a more detailed analysis, multiple regimes can be extended to the field inside the buffet with the additional aspects of: the establishment of modes, complex scattering due to the presence of hundreds or thousands

*gonzalo.villegas_curulla@upmc.fr; piergiovanni.domenighini@studenti.unipg.it; elliot.canfield-dafilou@dalembert.upmc.fr; benoit.fabre@sorbonne-universite.fr; christophe.dalessandro@sorbonne-universite.fr; brian.katz@sorbonne-universite.fr.

of pipes of different heights, and the establishment of a diffuse incident field onto the facade from the inside, where the facade constitutes the interface between the interior and the exterior of the organ buffet. This facade can be initially described as an array of air-masses trapped between cylinders (pipes) that are brought to oscillation.

In [6], the explicit problem of an evenly-distributed array of cylinders is discussed. These cylinders can represent organ pipes with known diameters and center-to-center spacing in the facade, where a first-order estimation is proposed to predict the scattered pressure. In [2], a comparative study of the 1-slit system was proposed using a laboratory proxy organ buffet, with respect to theoretical models informing directivity and full-range SPL-vs-frequency about the slit and the cylindrical source used in the current study of the positive.

The presence of the facade is bound to contribute as a frequency dependant boundary condition, resulting in a reflection or transmission with frequency dependant behaviour and with small losses. As a first approximation, it may well be considered almost transparent in the low frequencies. In [4], indices are shown that the protruding towers of the facade of the positive (see Section 1.1) constitute a scattering contribution already for the region of middle center frequencies of 1 kHz and 2 kHz.

1.1 The Organ in St. Élisabeth, Paris

The organ in St. Élisabeth was dedicated on 28 April, 1853 and restored in 1999. It is a large historical organ, with a total facade area of approximately $10\,\mathrm{m} \times 10\,\mathrm{m}$. The organ has three levels and hosts a total of 2322 pipes, of which 143 are visible in the facade. The organ has 42 stops on three manuals and pedal, with tracker action [7]. Figure 1 shows the locations of the three main radiating cavities and their wind-chest distributions.

The positive (420 pipes) stands on the floor of the organ loft, separated and in front of the main case and corresponds to the first manual keyboard. Its facade (inscribed in a $2.62\,\mathrm{m} \times 2.64\,\mathrm{m}$ surface) contains 33 pipes, organized in 3 towers of 5 pipes each, and 2 flat sets of 9 pipes. The tallest pipe in the facade is 6 feet, sounding F_1. It is relatively narrow and protrudes into the nave, radiating into free field without

(a) Facade.

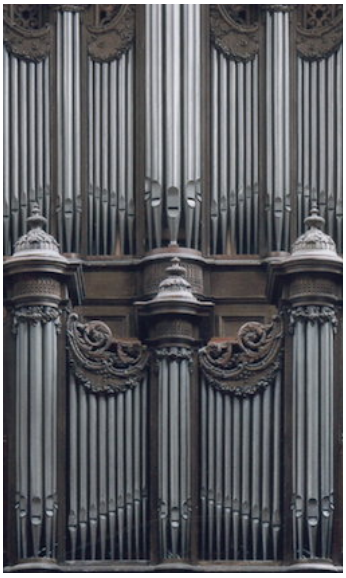

(b) Zoom on facade pipe details.

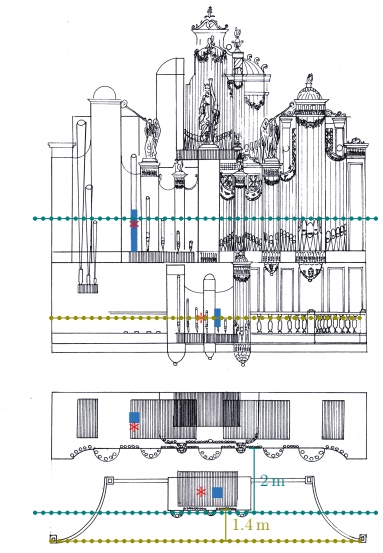

(c) Face (upper) and overhead (lower) views of the organ with position of the wind chests. 2D (■) and 3D (✳) source locations and receiver positions (–●–) are indicated.

Figure 1. The organ in St. Élisabeth, Paris and measurement schematics.

nearby reflective surfaces. Above the positive resides the main case 5.35 m above the floor level. It contains the *great organ* (GO) in the center, and the *pédale* on each sides behind the highest towers. The GO (1014 pipes) and pédale (180 pipes) correspond to the second manual keyboard and pedal board, respectively. Its facade is approximately 9.39 m × 9.6 m, and contains 75 pipes, organized in 7 towers and 8 flat segments. The tallest pipe in the facade is 12 feet (≈3.7 m), sounding F_0. The récit (708 pipes) crowns the instrument; it is enclosed in a swell-box and corresponds to the third manual keyboard. Its facade (inscribed in a 2.95 m × 3 m square) contains 35 mute pipes. The récit is not studied here.

The acoustics of the church show moderate reverberation times ($T_{20} = 2.14$ s to 3.68 s across the 125 Hz to 4000 Hz octave bands, see [8]).

1.2 Theory and Approximations

We make use of a number of approximations and assumptions in order to decompose the problem into smaller, less complex systems. Namely, we try to isolate and simplify the organ into studies on the sources, the pressure field inside the cavity, and the transmission and radiation into the building; the last of these being the subject of the current study. The sound-production sources are organ pipes with a non-flanged termination on one end (the so–called passive end of the resonator) and a mouth or window opening at the other end. The latter can be approximated in the low frequencies as a second monopole, but more elaborate characterizations are readily available: filtering has been described in [9] and general intensity around the pipe as a whole in [10]. The majority of pipes are assumed to be cylindrical and of open-open terminations. Each of them is not only a sound source, but also an obstacle to the propagation front of other sources within the buffet. In the condition of a fully closed buffet, the pressure field inside is mostly transmitted through the front face of the organ, the facade. The pipe-to-pipe spacings in the facade are the most salient transmission aperture outwards: they can be represented by an array of slits of resilient air-masses. Said slits are considered in the finite and infinitesimal thickness, and ideally as infinite in vertical length condition [6, 11, 12] or finite length, amounting to the full height of the cavity. These apertures become larger at the very bottom of the facade pipes due to the conicity of their foot, but this is considered irrelevant here. If acquisitions of the radiated field into the nave are made close enough to the facade, the infinitely tall slit [13] is a plausible approximation.

The effects of scattering will be expected to become apparent for $ka \gg 1$, where a is the half-width of the spacing between facade pipes, and $k = \omega/c$ is the wavenumber. For comparability purposes, the cavity of the St. Élisabeth's positive organ was chosen as a feasible approximation of the proxy organ used in previous laboratory studies [2, 3, 4].

2 Methods

The organ buffets under examination were excited by 6 s logarithmic sweeps spanning 60 Hz to 20 kHz, played from electroacoustic sources [14]. Signal acquisitions were made in several points inside the buffets for reference. The measurements outside the buffet were made along a set of equally-spaced locations in a straight line spanning the width of the nave (10 m). Acquisitions were made using the following audio hardware: RME UFX+, RME Octamic, omnidirectional measurement microphones BAMT1 class 1, and a Carver PM–175 Amplifier. The 3D source was a dodecahedron omnidirectional source, Dr. Three 3d-032. For the 2D cylindrical sources, the small 2D array was comprised of 18 Aurasound NSW2-326-8A speakers, with a 50 mm center-to-center spacing; the large 2D array was comprised of 10 Monacor SPH 165CP, with a 170 mm center-to-center spacing. The speakers were positioned near the center of the positive, and near the center of the left-half of the great organ. Groups of 4 to 5 microphones were arranged with 20 cm spacing on a transversal tension line, manually positioned using a pull-cord and measuring tape (see Figure 2(a)). See Figure 1(c) for source and receiver locations.

Deconvolution of the acquired signals was performed. Temporal alignment of the resulting IRs, compensating for arrival times, were calculated based on microphone positions along the acquisition lines, parallel to the measured facade (see Figure 1(c)), converting the linear measurement array to a polar propagation estimation relative to the source position. Octave-band frequency filtering of data was performed and relative pressure levels were calculated using fourth order Butterworth filters given by MATLAB's `octaveFilterBank`. Subsequent

(a) Transversal microphone measurement installation for the positive.

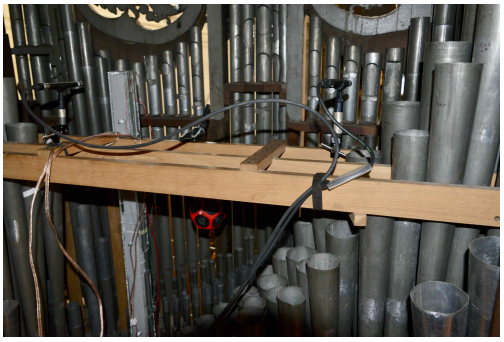

(b) 2D source configuration for the positive, showing 2D cylindrical source (left, grey column) and 3D omnidirectional source (centre, red).

(c) 2D source used in the GO, in the anechoic room.

Figure 2. Measurement setup example in St. Élisabeth and source.

amplitude correction of time aligned IRs was applied dependant on a reference distance r'/r, with r the shortest path at 0°. For the 3D omnidirectional source a -6 dB per doubling distance was employed. For the 2D cylindrical source, the correction was more complicated, employing a simplified model of -3 dB or -6 dB for near or far-field corrections, based on an idealized finite array (see [15]) with a $2L_c^2/\lambda$ rule for the cut-off, where L_c is a characteristic length, here the height of the source. The IRs were windowed in time to avoid contributions from from wall reflections. The length of this window was determined based on the distance between the microphones closest to the side-walls and the length of the direct path. An adequate estimation was determined to be 4.7 ms between the direct path to the microphone position closest to wall and its first reflection arrival, applied after time alignment of each position's deconvolved IR. Results are presented for octave bands from 125 Hz to 4 kHz. Due to the microphone spacing (20 cm), spatial aliasing limits the interpretability of higher frequency data.

3 RESULTS AND DISCUSSION

The octave band directivity pattern results for the positive are show in Figure 3, and for the GO in Figure 4, for the two source excitation conditions (3D omnidirectional and 2D cylindrical). Note the increasing measurement point density with increasing angle, due to the projection of the linear measurement setup to polar coordinates. Results are first examined for each buffet separately, then cross-compared. Closer inspection of the positive microphone array showed a variance in calibration level of 0.87 dB (B&K calibrator type 4231); accounting for this would likely resolve the observed minor fluctuations. Similar variations were not observed for the grand organ microphone array.

3.1 Positive Directivity

Inspection of the results for the positive identify a relatively omnidirectional directivity pattern across the octave band frequencies of 125 Hz to 1000 Hz (Figures 3(a) to 3(d)) for both 3D and 2D sources. Some minor attenuation can be observed at the extreme angles ($|\theta| > 50°$), likely due to the enclosure effect of the buffet windowing the energy generated within the buffet, redirecting it to the more central region. Patterns are relatively smooth, with measurement variations on the order of a few dB.

Directivity in the 2000 Hz octave band (Figure 3(e)) shows a significant broadening of the directivity for the 3D source, enforcing radiation at $\pm 45°$ relative to on-axis. This effect is less pronounced for the 2D source, where the directivity is more erratic compared to lower frequency bands. This effect is attributed to the significant scattering effect of the pipes and facade interface.

Results for the 4000 Hz octave band (Figure 3(f)) are similar to those at the low frequency bands, though with higher variance. This variance is expected due to the effects of spatial aliasing at higher frequencies.

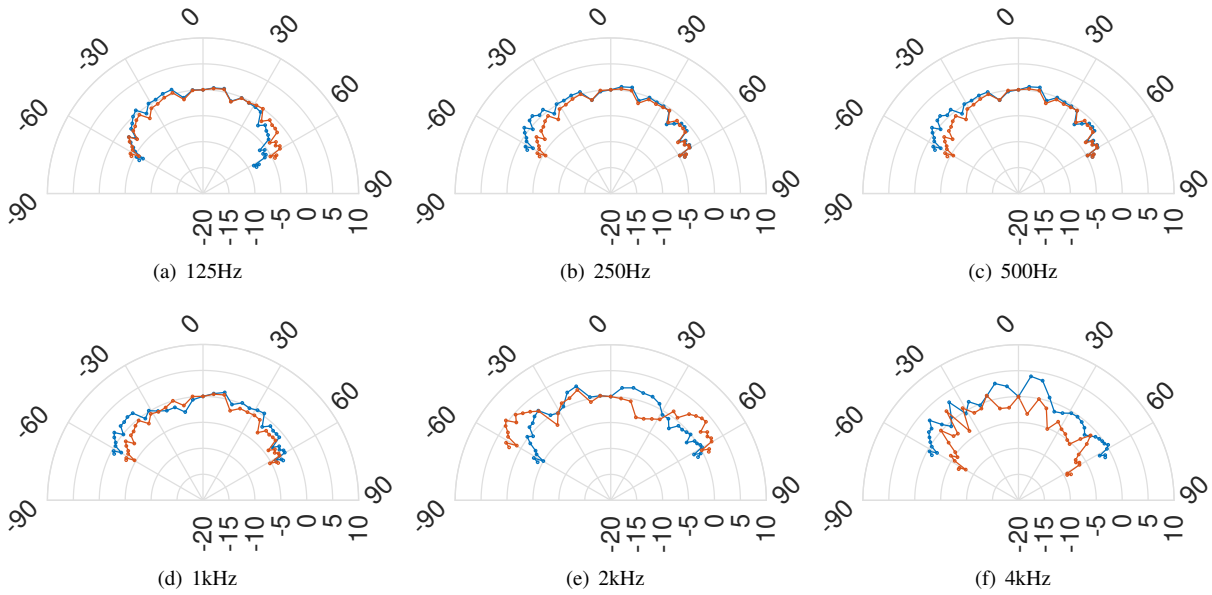

(a) 125Hz (b) 250Hz (c) 500Hz

(d) 1kHz (e) 2kHz (f) 4kHz

Figure 3. Directivity (dB) of positive organ for the 3D (—●—) and 2D (—●—) source excitation conditions, 4.7 ms window, and normalized to data at 0°.

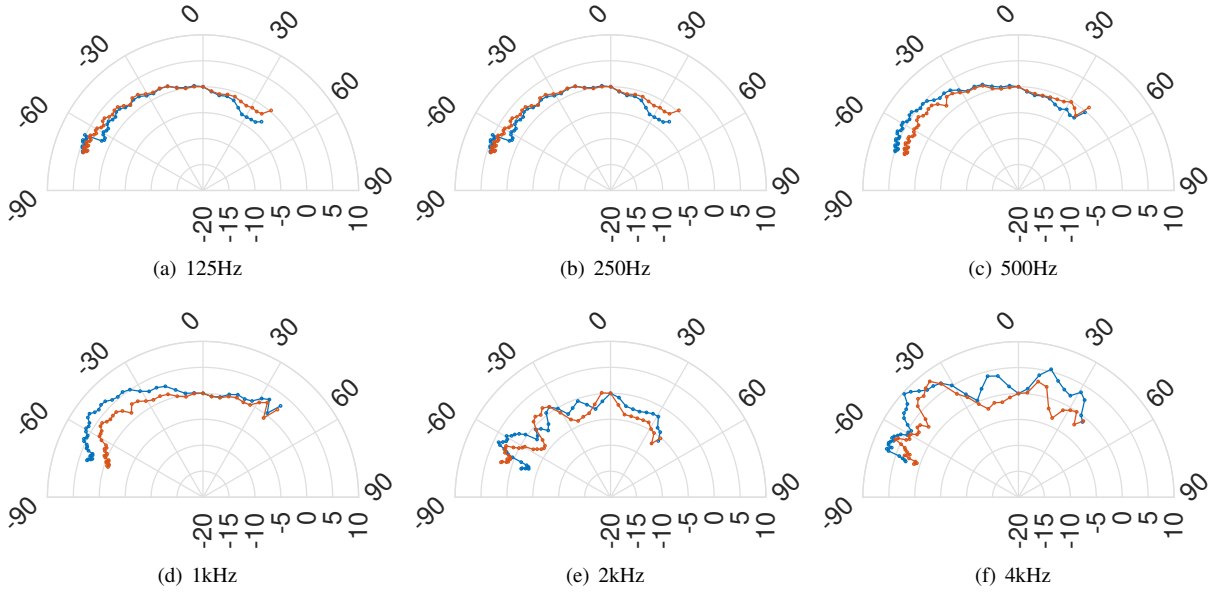

(a) 125Hz (b) 250Hz (c) 500Hz

(d) 1kHz (e) 2kHz (f) 4kHz

Figure 4. Directivity (dB) of the GO organ for the 3D (—●—) and 2D (—●—) source excitation conditions, 4.7 ms window, and normalized to data at 0°. Note the off-center position of the source relative to the building (see Figure 1(c), with the sources closer to the side wall (positive angles).)

3.2 Great Organ Directivity

Directivity patterns for the octave band frequencies of 125 Hz to 500 Hz (Figures 4(a) to 4(c)) show relatively omnidirectional directivity for both source types, with pattern fluctuations occurring at the extreme angles. The slight increase at the extreme ($\theta \geq 40°$) could be attributed to the contribution of minor reflections from the

side wall at such proximity to the boundary. At the other extreme positions ($\theta \gtrapprox -60$), one can observe an increase in energy relative to the on-axis response. For 125 Hz to 250 Hz, the 2D source directivity exhibits a discontinuity, likely attributed to the idealized cylindrical propagation correction for mapping the measurement points from their linear configuration to polar coordinates relative to the source position (see Section 2). A smoother, more sophisticated estimation of propagation properties for the truncated linear source array could improve results, though it is noted that the corrected values asymptotically converge to the 3D source response in those frequency bands. A general increase in energy is seen with negative angle progression (approaching 5 dB), more pronounced for 125 Hz to 250 Hz with the 3D source and 500 Hz with the 2D source.

Results for the 125 Hz to 1000 Hz octave bands (Figures 4(a) to 4(d)) show increasing emphasis for the extreme negative angles, (on the order of 5 dB). It is worth noting that the GO has horizontal platforms separating levels. It is plausible that with increasing angle, and hence increased distance to the receiver array, reflections from these floor/ceiling surfaces arrive with diminishing delays relative to the direct sound, thereby becoming more prevalent within the 4.7 ms analysis window. As this behavior appears common to both sources, this seems a reasonable assumption.

Results at the higher octave bands, 2000 Hz to 4000 Hz (Figures 4(e) to 4(f)), exhibit large oscillations in directivity patterns for both sources, though the patterns do not align at all angles. It would seem plausible that such variations in directivity could be attributed to the scattering properties of the large pipes making up the GO in general.

3.3 Positive and Great Organ Directivity Comparison

Comparing the results between the two measured organ buffets (the positive and GO), similar behaviour can be observed at the lower frequency regions, with markedly less measurement variance (noise) for the GO directivity patterns. This observation holds true for both sources, for which it is noted that the 3D was the same source while the 2D source was different due to the different dimensions/scale of the two organ buffets. For both buffets, the 2 kHz octave band showed the most pronounced deviations from free-field, omnidirectional directivity patterns, with patterns exhibiting increased variance at higher frequencies. The observed differences in these patterns between 3D and 2D sources suggest that the different excitation methods (spherical versus cylindrical waves) as well as the slight positional differences within the buffets and of the host of interior scatter objects induced different but still pronounced patterns.

While the GO contains more larger-diameter, low frequency pipes than the positive on the whole, examination of the two facades shows very similar pipe diameters in the center region (see Figure 1(b)), which would lead to an expectation of similar frequency behaviour with regards to scatter properties. However, while these patterns were clearly evident for the GO in the 2 kHz to 4 kHz octave bands, they are only observed in the 2 kHz octave band for the positive. The complex response of the positive could be attributed to the generally small pipe diameter and spacing within the buffet, producing scattered patterns with spatial resolutions exceeding the current measurements spatial aliasing limits. Reproducing these measurements with a finer spatial resolution would allow further investigation of this phenomenon at these frequency ranges.

4 CONCLUSIONS AND FUTURE WORK

This study has presented measurement results of an investigation into the diffraction/scattering effects of the organ buffet and facade on the directivity pattern of the radiated sound field. Two ideal sound sources were employed, an omnidirectional point source and a linear (truncated) cylindrical source, as approximations of an organ pipe source. Two sections of the church organ at St. Élisabeth were studied, the small and compact positive and the larger great organ. Measurements were made linearly, spanning the nave of the church at a distance of roughly 1.4 m to 2 m, and subsequently processed to obtain polar directivity data, excluding contributions of wall reflections through short time windowing.

Octave band results highlighted generally omnidirectional directivity in the frequency range of 125 Hz to 1000 Hz. Prominent variations were observed in the 2 kHz octave band, attributed to the diffraction and scattering effects of the pipes comprising the interior and facade of the organ. Similarity between the two organ sections in frequency appears reasonable as similar pipe dimensions are present in both the positive and great

organ, despite the presence of larger pipes in the great organ. Differences in the details of the pattern are expected due to differences in the pipes distribution patterns within the organ.

While some differences observed between the two excitation sources can be attributed predominantly to assumptions regarding corrections for near-field versus far-field propagation correction with the cylindrical source, these results suggest the source model is not a predominant factor in the directivity behaviour. Other variations are attributed to slight positional differences (not precisely coincident) of the two sources within the organ.

It is interesting to note that the dissymmetry in the GO patterns, due to the lateral position of the source excitation (particularly in the 1 kHz octave band), is consistent with the auditory perception of the diatonic disposition of the instrument. In St. Élisabeth, as is typical in large instruments, the wind-chests are diatonic, divided in C and C# sides. This means that half of the notes are on the left (in whole tones, C - D - E etc.) and half on the right (C# - D# - F etc.). This is contrary to, for instance, piano strings which are chromatically ordered (in semi-tones C - C# - D - D# etc.). This *ping-pong* effect is clearly audible (when one pays attention to it) and is part of the organ listening experience. Here, the sources were positioned on the C side of the organ. Directivity patterns suggest that the buffet may emphasize this effect by enhancing lateral perception.

Further studies shall examine the case using real organ pipe excitation sources within different regions of the organ, rather than the idealized electroacoustic sources in the current study, providing a more realistic context for the results [5]. These results could also be further enhanced by analyzing in finer frequency resolution, such as 1/3-octave bands and by exploration with finite difference and finite volume scheme simulations [16, 17], well-suited to scattering and diffraction problems.

Higher spatial resolution would be necessary to provide further conclusions regarding higher frequency bands. Such high resolution measurements have been carried out on a proxy organ, comparable to the positive of the current study, comprised of a homogeneous collection of simulated pipes and using the same sources [3, 4]. These studies examined in more detail the effect of pipe density in an attempt to simplify the diffraction/scattering problem.

The perceptual relevance of various organ properties in the context of auralizations is a primary application of the current results. Directivity perception is currently being evaluated through a series of listening tests, followed by a study which will examine the number of spatially distributed virtual sources required for plausible/-natural auralization renderings of the largest indoor musical instrument [18]. Such studies compliment previous works investigating the applicability of spatial perception metrics, such as the inter-aural cross correlation, as it pertains to the perceptual notion of *apparent source width* of such and extended instrument [8].

ACKNOWLEDGEMENTS

Funding for G.V.C. has been provided by the ISCD (grant no. FED 3 – 2019/7/2). Funding for E.C.D. and B.K. has been provided by the European Union's Joint Programming Initiative on Cultural Heritage project PHE (The Past Has Ears, phe.pasthasears.eu, Grant No. ANR-20-JPIC-0002), and the French project PHEND (The Past Has Ears at Notre-Dame, Grant No. ANR-20-CE38-0014, phend.pasthasears.eu, Grant No. ANR-20-CE38-0014).

REFERENCES

[1] Angster J, Rucz P, Miklos A. 25 years applied pipe organ research at Fraunhofer IBP in Stuttgart. In: Proc. Int. Symp. Musical Acoust. September; 2019. p. 1-14.

[2] Dal Moro P, Villegas Curulla G, Fabre B, d'Alessandro C. La boîte expressive de l'orgue: étude acoustique de la densité de tuyaux et d'une façade à ouverture variable. In: Proc. Congr. Fr. d'Acoust; 2022. p. 1-4. Available from: https://hal.archives-ouvertes.fr/hal-03673985.

[3] Villegas Curulla G, Dal Moro PMM, Fabre B, Katz BFG. Radiation patterns of a multiple slit system and applications to organ buffet modeling. In: Proc. Congr. Fr. d'Acoust.; 2022. p. 1-4. Available from: https://hal.archives-ouvertes.fr/hal-03700814.

[4] Villegas Curulla G, Domenighini P, Katz BFG, Canfield-Dafilou EK. Directivity of a small pipe organ buffet. In: Proc. Acoust. Ancient Theatres; 2022. p. 1-4. Available from: https://www.archives-ouvertes.fr/hal-03725002/.

[5] Villegas Curulla G, Domenighini P, Katz BFG, Canfield-Dafilou EK, Fabre B, d'Alessandro C. Preliminary analysis of organ buffet radiation under musically realistic excitation mechanism. In: Vienna Talk. Vienna; 2022. p. 1.

[6] Berry DL, Taherzadeh S, Attenborough K. Acoustic surface wave generation over rigid cylinder arrays on a rigid plane. J Acoust Soc Am. 2019;146(4):2137-44. doi:10.1121/1.5126856.

[7] d'Alessandro C. Orgues, Musiques et Musiciens à Sainte-Élisabeth. La flûte harmonique. 2010;(91):220. Available from: https://hal.archives-ouvertes.fr/hal-02360434.

[8] Katz BFG, d'Alessandro C. Apparent source width and the church organ. In: Proc. Congr. Fr. d'Acoust. and De. Gesellschaft Akust.; 2004. p. 1235-6. Available from: https://hal.archives-ouvertes.fr/hal-01789803.

[9] Ernoult A, Fabre B. Window impedance of recorder-like instruments. Acta Acustica united with Acustica. 2017;103(1):106-16. doi:10.3813/AAA.919037.

[10] Odya P, Kotus J, Szczodrak M, Kostek B. Sound Intensity Distribution Around Organ Pipe. Arch Acoust. 2017;42(1):13-22. doi:10.1515/aoa-2017-0002.

[11] Park HH, Eom HJ. Acoustic scattering from a rectangular aperture in a thick hard screen. J Acoust Soc Am. 1997;101(1):595-8. doi:10.1121/1.417971.

[12] Pàmies T, Romeu J, Genescà M, Balastegui A. Sound radiation from an aperture in a rectangular enclosure under low modal conditions. J Acoust Soc Am. 2011;130(1):239-48. doi:10.1121/1.3596465.

[13] Mellow T, Kärkkäinen L. On the sound fields of infinitely long strips. J Acoust Soc Am. 2011;130(1):153-67. doi:10.1121/1.3596474.

[14] Farina A. Advancements in impulse response measurements by sine sweeps. In: Audio Eng. Soc. Conv. 122. vol. 3; 2007. p. 1626-46.

[15] Chaigne A, Kergomard J. Acoustics of Musical Instruments. Springer; 2016.

[16] Bilbao S, Hamilton B. Passive Volumetric Time Domain Simulation for Room Acoustics Applications. J Acoust Soc of Am. 2018 10;145. doi:10.1121/1.5095876.

[17] Weber A, Katz BFG. Sound scattering by the Gothic piers and columns of the Cathédrale Notre-Dame de Paris. Acoustics. 2022;4:679-703. SI:Acoustics, Soundscapes and Sounds as Intangible Heritage. doi:10.3390/acoustics4030041.

[18] Canfield-Dafilou EK, Domenighini P, De Muynke J, d'Alessandro C, Katz BFG. Perceptual Influence of Directivity on Pipe Organ Auralization. In: Vienna Talk. Vienna; 2022. p. 1.